Mathematical modeling demonstrates how multiple slow processes can provide adjustable control of islet bursting

Margaret Watts,[1] Joel Tabak[2] and Richard Bertram[3,*]

[1]Department of Mathematics; [2]Department of Biological Science; [3]Department of Mathematics and Programs in Molecular Biophysics and Neuroscience; Florida State University; Tallahassee, FL USA

Pancreatic islets exhibit bursting oscillations that give rise to oscillatory Ca^{2+} entry and insulin secretion from β-cells. These oscillations are driven by a slowly activating K^+ current, K_{slow}, which is composed of two components: an ATP-sensitive K^+ current and a Ca^{2+}-activated K^+ current through SK4 channels. Using a mathematical model of pancreatic β-cells, we analyze how the factors that comprise K_{slow} can contribute to bursting. We employ the dominance factor technique developed recently to do this and demonstrate that the contributions that the slow processes make to bursting are non-obvious and often counter-intuitive, and that their contributions vary with parameter values and are thus adjustable.

Introduction

Pancreatic islets exhibit bursting oscillations, which consist of periodic episodes of electrical activity followed by quiescence. These oscillations are accompanied by oscillations in the free cytosolic Ca^{2+} concentration, which drives pulses of insulin secretion from β-cells.[1-3] Voltage clamp studies have shown that islet β-cells exhibit a slowly activating K^+ current, K_{slow}, that develops during simulated electrical activity and is Ca^{2+} dependent.[4,5] This current is not blocked by blockers of small-conductance (SK) or large-conductance (BK) Ca^{2+}-activated K^+ cannels, K(Ca), and has a single-channel conductance of an intermediate size. Later studies showed that roughly half of the K_{slow} current is mediated by a slow rise in the ATP-sensitive K^+, K(ATP), current.[6] Most recently, it was demonstrated that the other significant component of K_{slow} is mediated by SK4 Ca^{2+}-activated K^+, K(Ca), channels.[7] Thus, it appears that Ca^{2+} acts indirectly through K(ATP) and directly through SK4 to produce the K_{slow} current. Since this hyperpolarizing current builds up during repetitive burst-like spiking, it is likely the key current driving the so-called 'fast bursting' in islets.[8] Using a mathematical model of pancreatic β-cells,[9] we analyze how the factors that comprise K_{slow} can contribute to bursting. That is, the factors that start each burst and those that stop each burst. The model contains three variables that change on slow time scales: the cytosolic Ca^{2+} concentration, $[Ca^{2+}]_c$, endoplasmic reticulum (ER) Ca^{2+} concentration, $[Ca^{2+}]_{er}$, and the ratio of ADP to ATP (*a*). The ADP/ATP ratio determines the number of open K(ATP) channels; a larger ratio yields a larger K(ATP) conductance. This ratio is determined by the glucose concentration and, in part, by the cytosolic Ca^{2+}

concentration.[10-14] Thus, the contribution that the K(ATP) current makes to bursting is determined by the contribution that changes in the variable *a* make. Ca^{2+} acts directly to activate the SK4 channels, so SK4 conductance reflects the Ca^{2+} concentration in the cytosol, which in part reflects slow changes in the ER Ca^{2+} concentration.[15-17] Thus, the contribution that the SK4 current makes to bursting is determined by the contributions that changes in the variables $[Ca^{2+}]_c$ and $[Ca^{2+}]_{er}$ make.

The Ca^{2+} in the ER affects the membrane in several potential ways. First, it acts as a filter for Ca^{2+} from the cytosol, taking up Ca^{2+} when the cell is spiking and $[Ca^{2+}]_c$ is elevated and releasing Ca^{2+} during the silent phase of a burst when $[Ca^{2+}]_c$ is at a low value.[15-17] This effect is incorporated into our model. Second, the ER releases Ca^{2+} into the cytosol when inositol-1,4,5-trisphosphate $[Ins(1,4,5)P_3]$ receptors or ryanodine receptors in the ER membrane are activated. This Ca^{2+} release can directly affect the membrane through actions on Ca^{2+}-activated K^+ channels and indirectly through effects on the ADP/ATP ratio. Finally, the subsequent decline in $[Ca^{2+}]_{er}$ can activate store operated current (reviewed in ref. 18). In the model, we assume that no $Ins(1,4,5)P_3$ or ryanodine receptor agonists are present.

In this paper, we examine how the two components of K_{slow} can contribute to bursting, and demonstrate with the model that their contributions can vary in non-obvious ways depending on the maximal conductances of the K(ATP) and SK4 currents, as well as the time scales of the slow variables. We employ the dominance factor technique developed recently to quantify the contributions made by the slow variables to bursting.[19] The model that we use is one of many that have been developed for pancreatic β-cells.[20-35] The dominance factor technique can be applied to
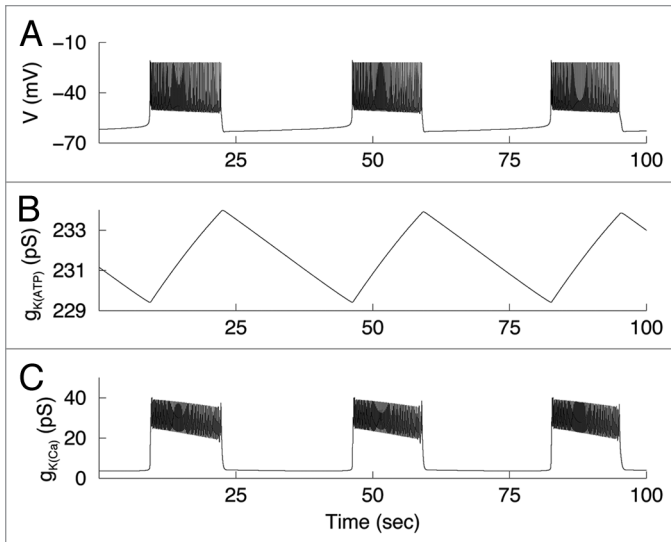
Figure 1. Time-dependent membrane potential (A) and conductances of the K(ATP) (B) and K(Ca) (C) currents. The K(ATP) conductance (B) is always larger than the K(Ca) conductance (C). However, the change in the K(Ca) conductance is greater than the change in the K(ATP) conductance.

most of these, which have more than one slow variable acting on the membrane potential.

Results

K$_{slow}$ conductances reveal little about the control of bursting. Our aim is to understand how the components of K$_{slow}$ can contribute to bursting. Can we determine which component starts and stops each burst by looking at the conductances? **Figure 1** shows the model conductances for the K(ATP) ($g_{K(ATP)}$) (**Fig. 1B**) and SK4 ($g_{K(Ca)}$) currents (**Fig. 1C**). The K(ATP) conductance is always larger than the SK4 conductance, so one might conclude that the K(ATP) current controls both phases of bursting. Certainly, if this current were blocked the model cell would not burst, but would spike continuously. However, this does not mean that the time-dependent variation in the K(ATP) conductance plays a role in starting and stopping the bursts. If instead one looked only at the amplitude of the conductance variations, one would reach the opposite conclusion, since the amplitude of the SK4 conductance variation (~40 pS) is much greater than that of the K(ATP) conductance variation (~4 pS). Of course, the K(ATP) conductance varies on the time scale of the burst, while the SK4 current enters and leaves its elevated plateau on a much shorter timescale. Therefore, one might again conclude that the K(ATP) current controls the bursting. Clearly then, even if the conductances were known at time points throughout the burst, it would not be obvious how to use this information to understand what turns the bursts on and off. This ambiguity motivates the different approach that we use.

Slow processes differentially regulate the phases of bursting. Bursting electrical oscillations are driven by the gradual buildup and decline of one or more slow processes. Each of these processes

is represented by a "slow variable" in mathematical models. The mathematical model we use[9] contains three slow variables: the Ca^{2+} concentration in the cytosol, $[Ca^{2+}]_c$, and in the endoplasmic reticulum, $[Ca^{2+}]_{er}$, and the ratio of ADP to ATP (a). The K(ATP) current is proportional to a:

$$I_{K(ATP)} = \bar{g}_{K(ATP)}a(V - V_K) \tag{1}$$

where $\bar{g}_{K(ATP)}$ is the maximal conductance of the channels and V_K is the K$^+$ Nernst potential. The SK4 current depends on $[Ca^{2+}]_c$,

$$I_{K(Ca)} = \bar{g}_{K(Ca)}\omega(V - V_K) \quad \text{where } \omega = \frac{[Ca^{2+}]_c^5}{k_D^5 + [Ca^{2+}]_c^5} \tag{2}.$$

The cytosolic Ca^{2+} concentration is determined by Ca^{2+} influx and pumping through the plasma membrane, and cycling of Ca^{2+} into and out of the ER. It is through this latter pathway that the Ca^{2+} concentration in the ER affects $[Ca^{2+}]_c$, which in turn influences a due to ATP utilization by pumps (see Eq. 12 in Materials and Methods).[12] Therefore, instead of looking at the conductances, we look at the dynamics of the slow variables which underlie the conductances.

Bursting oscillations with different periods are produced for different values of the maximal conductance of the SK4 current ($\bar{g}_{K(Ca)}$) in the model. This maximal conductance is the conductance when all K(Ca) channels in the cell are open. **Figure 2** shows bursting obtained with the model for two different values of $\bar{g}_{K(Ca)}$. The left column (A–D) shows bursting with a high value of $\bar{g}_{K(Ca)}$ (1,500 pS). In this case, the bursting has a period of ~1 sec (**Fig. 2A**), and $[Ca^{2+}]_c$ increases during the active and decreases during the silent phase of the burst (**Fig. 2B**). However, $[Ca^{2+}]_{er}$ and a are almost constant since they change slowly and the bursts are very short (**Fig. 2C and D**). In this case, it is clear that variations in $[Ca^{2+}]_c$ control the termination of both the active and silent phases of the burst. For a low value of $\bar{g}_{K(Ca)}$ (500 pS), the burst period is ~70 sec (**Fig. 2E**). $[Ca^{2+}]_c$ quickly reaches a plateau during the active phase and has a component that quickly declines during the silent phase (**Fig. 2F**). A second component reflects the dynamics of ER Ca^{2+} handling.[15-17] The other two slow variables, $[Ca^{2+}]_{er}$ and a, exhibit saw tooth-like oscillations that are characteristic of variables that drive bursting.[36] Thus, $[Ca^{2+}]_{er}$ and a likely play large roles in the bursting oscillation. How large? Do they contribute differentially to the active and silent phases?

Using the method of quantification described in Watts et al. we determine the contributions that each of the three slow variables make to bursting for different values of $\bar{g}_{K(Ca)}$ (Eq. 17 in Materials and Methods). Briefly, the contribution of the variable to the termination of the active phase and silent phase is determined by increasing the time constant for one of the slow variables at the beginning of the phase. This increase in the time constant slows down the variable, and if the activity-dependent change in this variable contributes to the termination of the phase, then the phase duration increases.[37]

Figure 3 shows the contribution that each slow variable makes to the termination of the active and silent phases of bursting. As $\bar{g}_{K(Ca)}$ is increased, the period of bursting decreases (**Fig. 3A**). **Figure 3B** shows the contribution factors of the slow variables for the termination of the active phase. For low values of $\bar{g}_{K(Ca)}$, $[Ca^{2+}]_{er}$ (gray bar) and a (black bar) both contribute to the termination of the active phase. As $\bar{g}_{K(Ca)}$ is increased, the contribution of a declines (the black bar gets smaller). For even larger values of $\bar{g}_{K(Ca)}$, $[Ca^{2+}]_c$ is the only sole variable contributing to active phase termination (white bar). This shift in control from $[Ca^{2+}]_{er}$ and a to $[Ca^{2+}]_c$ is expected since increasing $\bar{g}_{K(Ca)}$ accentuates the Ca^{2+}-activated K^+ current. Similarly, **Figure 3C** shows the contribution factors for the termination of the silent phase. The contributions of a and $[Ca^{2+}]_{er}$ start out equal for low values of $\bar{g}_{K(Ca)}$, then a gains control as $\bar{g}_{K(Ca)}$ is increased. This is unexpected; increasing $\bar{g}_{K(Ca)}$ actually leads to an increase in the role played by the ADP/ATP ratio to bursting. Only when $\bar{g}_{K(Ca)}$ >1,100 pS does $[Ca^{2+}]_c$ gain control of the silent phase, as it does for the active phase. Therefore, for low values of $\bar{g}_{K(Ca)}$ both phases of bursting are controlled by $[Ca^{2+}]_{er}$ and a, while for high values of $\bar{g}_{K(Ca)}$, the direct feedback of Ca^{2+} onto SK4 channels is the only component of K_{slow} contributing to bursting in the model.

One way to summarize the relative contributions to bursting of two slow variables (such as $[Ca^{2+}]_{er}$ and a for small values of $\bar{g}_{K(Ca)}$) is to use a measure called the dominance factor (DF) for each phase (Eq. 18 of Materials and Methods). A dominance factor of 1 indicates that $[Ca^{2+}]_{er}$ dominates, while a dominance factor of -1 indicates that a dominates. The results using the dominance factor are shown in **Figure 4**. As $\bar{g}_{K(Ca)}$ is increased, the period of bursting decreases (**Fig. 4A**). Also, control of the termination of the active phase switches from mostly a to mostly $[Ca^{2+}]_{er}$. Control of the silent phase shows the opposite trend, from equal contributions at low $\bar{g}_{K(Ca)}$ to mostly controlled by a for higher values of $\bar{g}_{K(Ca)}$ (**Fig. 4B**). It appears, then, that the control of the active and silent phases is not linked; one slow variable can primarily control the active phase while another can primarily control the silent phase. The distribution of control varies with SK4 channel conductance, and thus burst period.

Effect of parameters on the dominance factor. The contribution that the slow variables make to bursting depends upon parameter values. **Figure 4** demonstrated how control over the termination of the active and silent phases changed as $\bar{g}_{K(Ca)}$ was varied. In **Figure 5** we show the effect of varying $\bar{g}_{K(ATP)}$ on the dominance factors (while fixing $\bar{g}_{K(Ca)}$). As $\bar{g}_{K(ATP)}$ is increased the duration of the silent phase also increases (black dots), while the duration of the active phase decreases (white dots) slightly (**Fig. 5A**). Likewise, the dominance factor for the silent phase increases with $\bar{g}_{K(ATP)}$, but the dominance factor for the active
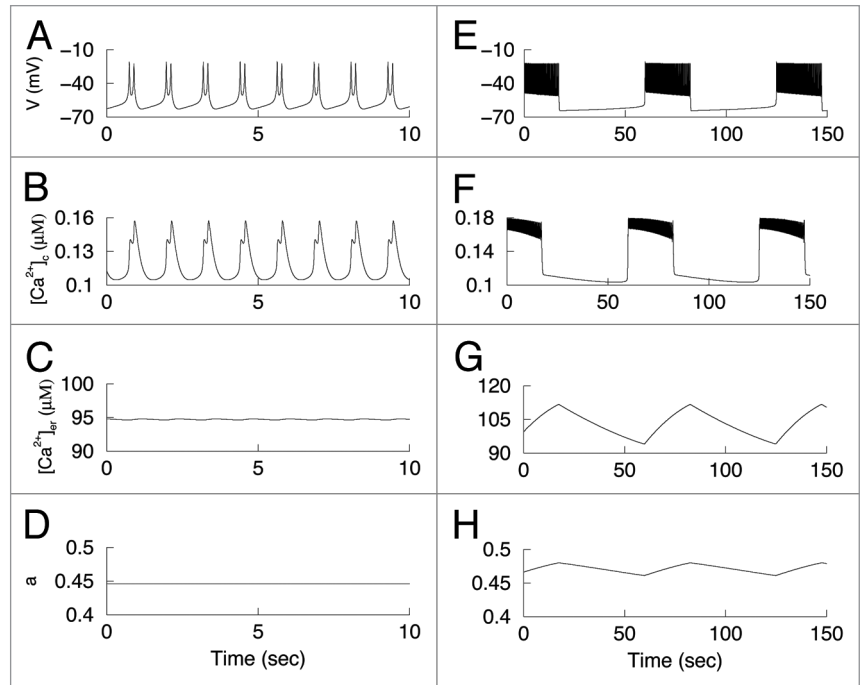
Figure 2. Bursting with $[Ca^{2+}]_c$ in control, $\bar{g}_{K(Ca)} = 1,500$ pS (A–D). $[Ca^{2+}]_c$ is increasing during the active phase and decreasing during the silent phase (B), while $[Ca^{2+}]_{er}$ (C) and a (D) remain constant. Bursting with $[Ca^{2+}]_{er}$ and a sharing control, $\bar{g}_{K(Ca)} = 500$ pS (E–H). $[Ca^{2+}]_c$ quickly reaches its maximum during the active phase and its minimum during the silent phase (F), but $[Ca^{2+}]_{er}$ (G) and a (H) slowly increase during the active phase and decrease during the silent phase. Notice the much longer time scale for this latter form of bursting. In all cases, $\bar{g}_{K(ATP)} = 500$ pS.

phase decreases (**Fig. 5C**). This is surprising, since one might expect that increasing the maximal conductance for the K(ATP) current would give a more control over both the silent phase and active phase, but it partially loses control of the silent phase. It is interesting to note that the silent phase also acted in a nonintuitive way when $\bar{g}_{K(Ca)}$ was increased (**Fig. 4B**). With $\bar{g}_{K(Ca)}$ set to a higher value (700 pS) so that the bursting was much faster, increasing $\bar{g}_{K(ATP)}$ had a similar effect on the dominance factors (**Fig. 5B and D**). The duration of the silent phase rises significantly with the increase of $\bar{g}_{K(ATP)}$, as does the dominance factor. The duration of the active phase changes little, yet there is a substantial shift of control from mostly $[Ca^{2+}]_{er}$ to equal contributions of $[Ca^{2+}]_{er}$ and a.

Other parameters that affect the contribution and dominance factors are the time constants of the slow variables. These parameters determine how rapidly the variables change (a large time constant τ means a slow rate of change). **Figure 6A** shows the effect on the dominance factor of increasing the time constant for a (τ_a) with $\bar{g}_{K(Ca)} = 600$ pS and $\bar{g}_{K(ATP)} = 500$ pS. As τ_a is increased a becomes slower and contributes less to the termination of the active phase (white bars) and silent phase (gray bars). It is interesting to note that a always has substantial influence over the silent phase, even when τ_a is very large. **Figure 6B** shows the effect of increasing τ_{er}. As τ_{er} is increased, $[Ca^{2+}]_{er}$ gets slower and the dominance factor decreases. Therefore, a gains control over both the active phase (white bars) and silent phase (gray bars).
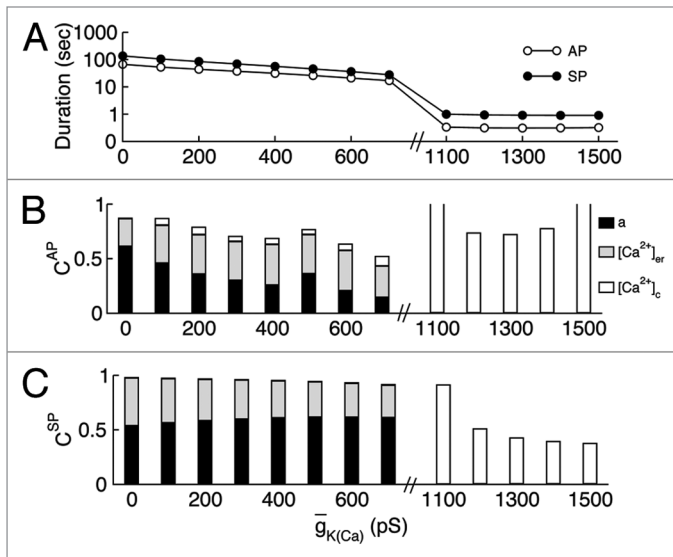
Figure 3. Slow variable contributions to the active and silent phases of bursting. (A) The durations of the active and silent phases decrease as $\bar{g}_{K(Ca)}$ is increased. (B) Contribution factors for the three slow variables: $[Ca^{2+}]_c$, $[Ca^{2+}]_{er}$, and a to the termination of the AP. (C) Contribution factors for the termination of the SP. For low values of $\bar{g}_{K(Ca)}$, $[Ca^{2+}]_{er}$ and a share control of the bursting. However, for high values of $\bar{g}_{K(Ca)}$, $[Ca^{2+}]_c$ is in control of both the active and silent phases. For some values of $\bar{g}_{K(Ca)}$ the contribution factor was greater than 1 and the bar is cut off.
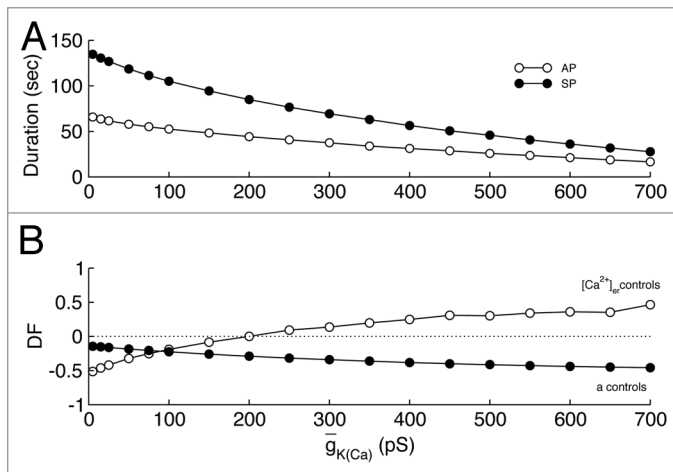
Figure 4. Using the dominance factor to analyze the control of bursting. (A) As $\bar{g}_{K(Ca)}$ is increased, the duration of both the active and silent phases decreases. (B) As $\bar{g}_{K(Ca)}$ is increased, the active phase dominance factor (DF) increases, while the silent phase DF decreases. For the AP, control shifts from a to $[Ca^{2+}]_{er}$, while a is always primarily responsible for the SP duration ($\bar{g}_{K(ATP)} = 500$ pS).

Discussion

Using a mathematical model of the pancreatic β-cell,[9] we addressed the question of how the two known components of the K_{slow} current can contribute to bursting oscillations in islets. We first argued that the time-dependent conductances of the

currents provide ambiguous information about the control of bursting. A better approach is to examine the variables that underlie the conductances. Using an analysis technique developed earlier in reference 19, we showed that control of the phases of bursting is adjustable. In particular, it depends on the values of maximal conductances and the rate of change of the variables underlying the currents. We showed that for low values of $\bar{g}_{K(Ca)}$, $[Ca^{2+}]_{er}$ and a shared control of the bursting, in other words, both the active phase and silent phase duration were affected similarly by a change in the time constants of a and $[Ca^{2+}]_{er}$, while for larger values $[Ca^{2+}]_c$ had control (**Fig. 3**). We also showed that the active and silent phases of bursting do not have to be controlled by the same variable (**Fig. 4**). For example, when $\bar{g}_{K(Ca)} = 700$ pS and $\bar{g}_{K(ATP)} = 500$ pS, the active phase is mostly controlled by $[Ca^{2+}]_{er}$, while the silent phase is mostly controlled by a. This situation is altered when $\bar{g}_{K(Ca)}$ is much lower (25 pS), in which case the active phase is mostly controlled by a and both a and $[Ca^{2+}]_{er}$ control the silent phase.

We also show that as parameters are varied, the contributions of a and $[Ca^{2+}]_{er}$ change in non-intuitive ways. As $\bar{g}_{K(Ca)}$ is increased, a gains more control over the silent phase. As $\bar{g}_{K(ATP)}$ is increased, $[Ca^{2+}]_{er}$ gains more control over the silent phase. Understanding the basis for these non-intuitive results requires an analysis of how the slow variables act on the fast variables such as voltage. This type of analysis was used previously to examine a simpler model for β-cell bursting.[19]

Our results could not have been obtained by looking at the conductances of the channels; a different approach had to be used. It is also difficult or impossible to do this analysis experimentally, since it requires an acute increase in the time constants that are typically not controllable. This highlights one advantage of mathematical models, where all parameters are controllable. Parameters that can be modified in the lab through pharmacological means, such as the ionic conductances, may also change the burst mechanism (**Figs. 3–5**). However, one could not tell just by looking at the voltage trace. For example, **Figure 4A** shows a quantitative change in the durations of the active and silent phases of bursting as $\bar{g}_{K(Ca)}$ is increased. This can be seen experimentally. However, the dominance factor also changes (**Fig. 4B**), reflecting a modification of the burst mechanism. As another example, **Figure 5B** shows little change in the active phase duration as $\bar{g}_{K(ATP)}$ is varied, yet control of the active phase shifted from mostly $[Ca^{2+}]_{er}$ to equal contributions from $[Ca^{2+}]_{er}$ and a. These changes would be hard to see without the aid of a mathematical model.

It has been shown that islet bursting can be fast, slow or compound. There is a great deal of evidence for a metabolic oscillator that is responsible for slow bursting and for packaging fast bursts into episodes during compound bursting. This is described by the Dual Oscillator Model.[8] Here we have focused on fast bursting, so our model does not include the machinery for glycolytic oscillations. Also, some islets exhibit endogenous metabolic oscillations, while others do not.[38] Those that do not can exhibit fast bursting, but in some cases a change in the glucose concentration can convert the fast bursts to compound bursts, presumably due to activation of the glycolytic

oscillator.[39] When glycolytic oscillations are present, the model variable a will vary periodically due to this endogenous oscillation, but will also retain its dependence of Ca^{2+}. Thus, the analysis presented here should be thought of as an investigation of fast bursting that stands alone or is part of a compound oscillation.

The dominance factor technique applied here could be applied to any β-cell model with more than one slow variable. Examples include the recent models of Diederichs[20] and Fridlyand.[21,22] The many models developed over the past three decades[20-35] are simplifications of actual β-cells, which have many ionic currents and signaling pathways and are very heterogeneous.[40,41] Yet, these models can reveal dynamic interactions that are hard to extract from the data alone. In this report, we demonstrate that the slow processes underlying the K_{slow} current collaborate in burst production. The quantitative relationship of these processes to burst production varies with parameter values and undoubtedly varies between models. However, the central point of adjustable collaboration to burst production should be valid for models that are more complex than the one used here.

Materials and Methods

Mathematical model. We use a relatively simple model of pancreatic β-cells[9] which consists of a Ca^{2+} current, I_{Ca}, a delayed rectifier K^+ current, I_K, a Ca^{2+}-dependent K^+ current (SK4), $I_{K(Ca)}$, and a nucleotide-sensitive K^+ current, $I_{K(ATP)}$. The differential equations for membrane potential, V, delayed rectifier activation, n, cytosolic free Ca^{2+} concentration, $[Ca^{2+}]_c$, ER Ca^{2+} concentration, $[Ca^{2+}]_{er}$, and the ADP/ATP ratio, a, are as follows:

$$\frac{dV}{dt} = -[I_{Ca} + I_K + I_{K(Ca)} + I_{K(ATP)}]/C_m \quad (3)$$

$$\frac{dn}{dt} = (n_\infty - n)/\tau_n \quad (4)$$

$$\frac{d[Ca^{2+}]_c}{dt} = ([Ca^{2+}]_{c\infty} - [Ca^{2+}]_c)/\tau_c \quad (5)$$

$$\frac{d[Ca^{2+}]_{er}}{dt} = ([Ca^{2+}]_{er\infty} - [Ca^{2+}]_{er})/\tau_{er} \quad (6)$$

$$\frac{da}{dt} = (a_\infty([Ca^{2+}]_c) - a)/\tau_a \quad (7)$$

with ionic currents:
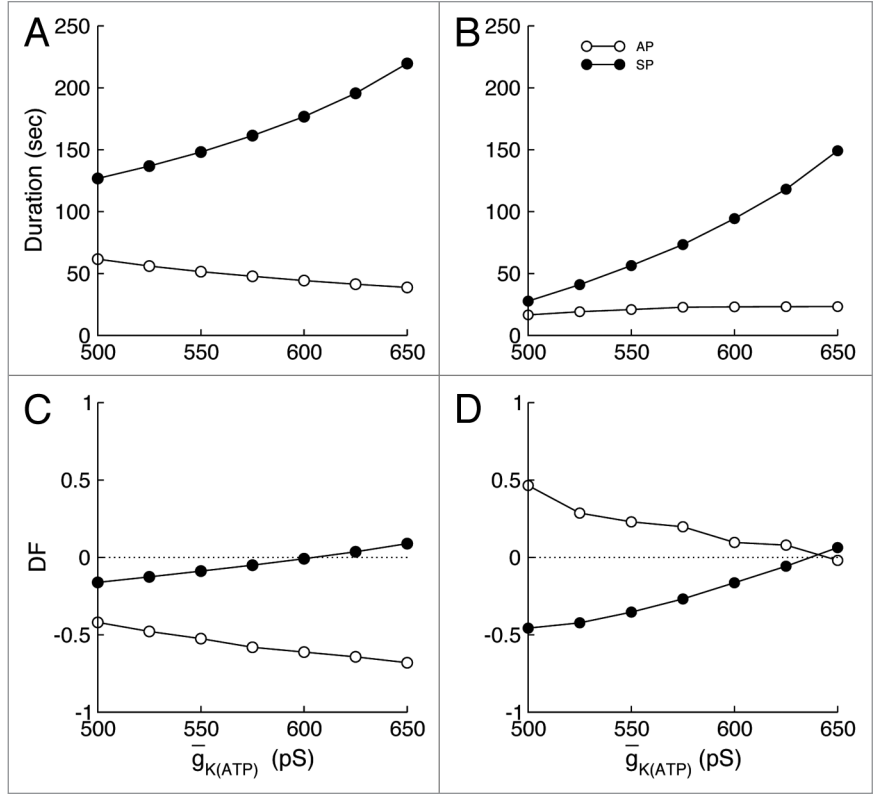
Figure 5. Changes in durations and the dominance factors while changing $\bar{g}_{K(ATP)}$ and keeping $\bar{g}_{K(Ca)}$ constant. (A and B) As $\bar{g}_{K(ATP)}$ is increased, the SP duration increases, while the AP duration decreases. (C and D) As $\bar{g}_{K(ATP)}$ is increased, the active phase DF decreases, while the silent phase DF increases. ($\bar{g}_{K(Ca)}$ = 25 pS for A and C, while $\bar{g}_{K(Ca)}$ = 700 pS for B and D).

$$I_{Ca} = \bar{g}_{Ca} m_\infty(V)(V - V_{Ca}), \quad I_K = \bar{g}_K n(V - V_K) \quad (8)$$

$$I_{K(Ca)} = \bar{g}_{K(Ca)}\omega(V - V_K), \quad I_{K(ATP)} = \bar{g}_{K(ATP)}a(V - V_K) \quad (9).$$

C_m is the membrane capacitance, the $\bar{g}$ parameters are the maximal conductances, the τ parameters are time constants, and V_{Ca} and V_K are reversal potentials. The variable ω is the fraction of K(Ca) channels activated by cytosolic Ca^{2+}:

$$\omega = \frac{[Ca^{2+}]_c^5}{[Ca^{2+}]_c^5 + k_D^5} \quad (10).$$

The steady-state activation functions depend on voltage:

$$m_\infty(V) = [1 + e^{(v_m - V)/s_m}]^{-1}, \quad n_\infty(V) = [1 + e^{(v_n - V)/s_n}]^{-1} \quad (11).$$

The equilibrium function, $a_\infty([Ca^{2+}]_c)$, depends on the cytosolic Ca^{2+} concentration:
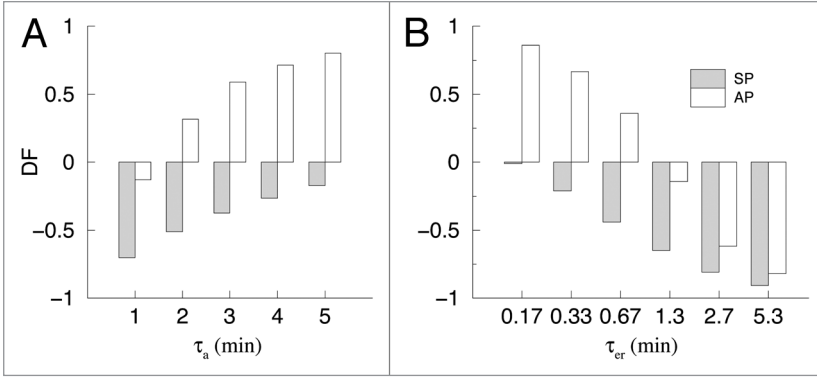
Figure 6. (A) Effect of changing the time constant τ_a on the DF. As τ_a increases, the DF increases for both the AP and SP, indicating that a loses control. The default value of τ_a is 2 min. (B) Effect of changing τ_{er} on the DF. As, τ_{er} increases, the DF decreases for both the active and silent phases, indicating that a is gaining control. The default value of τ_{er} is 0.67 min. In both parts, $\bar{g}_{K(Ca)} = 600$ pS and $\bar{g}_{K(ATP)} = 500$ pS.

Table 1. Parameter values for the model

Parameter	Value	Parameter	Value
$\bar{g}_{Ca}$	1,200 pS	$\bar{g}_K$	3,000 pS
V_{Ca}	25 mV	V_K	-75 mV
C_m	5,300 fF	α	4.5×10^{-6} fA^{-1}μM ms^{-1}
τ_n	16 ms	τ_a	120,000 ms
f_{cyt}	0.01	f_{er}	0.01
k_{PMCA}	0.2 ms^{-1}	k_D	0.3 μM
v_n	-16 mV	s_n	5 mV
v_m	-20 mV	s_m	12 mV
k_{SERCA}	0.4 ms^{-1}	p_{leak}	0.0005 ms^{-1}
V_{cyt}/V_{er}	5	s_a	0.1 μM
r	0.14	$\bar{g}_{K(ATP)}$	500 pS

$$a_\infty([Ca^{2+}]_c) = [1 + e^{(r-[Ca^{2+}]_c)/s_a}]^{-1} \qquad (12).$$

The equilibrium functions $[Ca^{2+}]_{c\infty}$ and $[Ca^{2+}]_{er\infty}$ are given by:

$$[Ca^{2+}]_{c\infty} = \frac{p_{leak}[Ca^{2+}]_{er} - \alpha I_{Ca}}{k_{PMCA} + p_{leak} + k_{SERCA}} \qquad (13)$$

$$[Ca^{2+}]_{er\infty} = [Ca^{2+}]_c (1 + \frac{k_{SERCA}}{p_{leak}}) \qquad (14),$$

where α converts units of current to units of flux, k_{PMCA} is the pump rate of the plasma membrane Ca^{2+} ATPase pumps, k_{SERCA} is the pump rate for SERCA pumps, and p_{leak} is the Ca^{2+} leak out of the ER. Lastly, the time constants for cytosolic and ER Ca^{2+} concentrations are:

$$\tau_c = \frac{1}{f_{cyt}(k_{PMCA} + p_{leak} + k_{SERCA})} \qquad (15)$$

$$\tau_{er} = \frac{V_{er}}{f_{er}V_{cyt}p_{leak}} \qquad (16),$$

where f_{cyt} and f_{er} are the fractions of free Ca^{2+} in the cytosol and ER, respectively, and V_{cyt} and V_{er} are the volumes of the cytoplasmic and ER compartments. Parameter values are given in **Table 1**. Model equations were solved numerically using the CVODE algorithm implemented in the XPPAUT software package.[42] Computer codes are available as freeware from www.math.fsu.edu/~bertram/software/islet.

Contribution factors and dominance factors. The method used to quantify the contribution that a slow process makes to bursting was described previously in reference 19. Briefly, we determine the contribution that each slow variable makes to the active (AP) and silent (SP) phases of bursting by increasing the time constant, τ_x, for one of the slow variables at the beginning of the phase by $\delta\tau_x$. This increase in the time constant slows down the slow variable, and if the activity-dependent change in this variable contributes to the termination point of the phase, then the phase should increase by values δAP or δSP. The contribution of the slow variable, x, to the active phase and silent phase durations is given by:

$$C_{AP}^x = \left(\frac{\delta AP}{\delta\tau_x}\right)\left(\frac{\tau_x}{AP}\right), \quad C_{SP}^x = \left(\frac{\delta SP}{\delta\tau_x}\right)\left(\frac{\tau_x}{SP}\right) \qquad (17),$$

where AP and SP are active and silent phase durations, respectively. Larger values of C indicate larger contributions. Here we used $\delta\tau_x = \tau_x$ for the active phase and $\delta\tau_x = 0.1\tau_x$ for the silent phase.

For small values of $\bar{g}_{K(Ca)}$, $[Ca^{2+}]_{er}$ and a are the only slow variables contributing to bursting (**Fig. 3**). By comparing the C values of these two slow variables, we can evaluate the relative contributions of $[Ca^{2+}]_{er}$ and a to active phase and silent phase durations. This is facilitated by using a measure called the dominance factor (DF) for each phase:[19]

$$DF_{AP} = \frac{C_{AP}^{er} - C_{AP}^a}{\sqrt{(C_{AP}^{er})^2 + (C_{AP}^a)^2}}, \quad DF_{SP} = \frac{C_{SP}^{er} - C_{SP}^a}{\sqrt{(C_{SP}^{er})^2 + (C_{SP}^a)^2}} \qquad (18).$$

Defined this way, the dominance factor should be between -1 and 1. A dominance factor of 1 indicates that $[Ca^{2+}]_{er}$ dominates, while a dominance factor of -1 indicates that a dominates.

References

1. Gilon P, Henquin JC. Influence of membrane potential changes on cytoplasmic Ca^{2+} concentration in an electrically excitable cell, the insulin-secreting pancreatic B-cell. J Biol Chem 1992; 267:20713-20; PMID:1400388.

2. Bergstein P. Slow and fast oscillations of cytosolic Ca^{2+} correspond to pulsatile insulin release. Am J Physiol 1995; 268:282-7; PMID:7864105.

3. Barbosa RM, Silva AM, Tome AR, Stamford JA, Santos RM, Rosario LM. Control of pulsatile 5-HT/insulin secretion from single mouse pancreatic islets by intracellular calcium dynamics. J Physiol 1998; 510:135-43; PMID:9625872; DOI:10.1111/j.1469-7793.1998.135bz.x.

4. Gopel SO, Kanno T, Barg S, Eliasson L, Galcanovskis J, Renstrom E, et al. Activation of Ca^{2+}-dependent K^+ channels contributes to rhythmic firing of action potentials in mouse pancreatic β cells. J Gen Physiol 1999; 114:759-70; PMID:10578013; DOI:10.1085/jgp.114.6.759.

5. Goforth PB, Bertram R, Khan FA, Zhang M, Satin LS. Calcium-activated K^+ channels of mouse β-cells are controlled by both store and cytoplasmic Ca^{2+}: Experimental and theoretical studies. J Gen Physiol 2002; 120:307-22; PMID:12198088; DOI:10.1085/jgp.20028581.

6. Kanno T, Rorsman K, Gopel SP. Glucose-dependent regulation of rhythmic action potential firing in pancreatic β-cells by K_{ATP}-channel modulation. J Physiol 2002; 545:501-7; PMID:12456829; DOI:10.1113/jphysiol.2002.031344.

7. Düfer M, Gier B, Wolpers D, Krippeit-Drews P, Ruth P, Drews G. Enhanced glucose tolerance by SK4 channel inhibition in pancreatic β-cells. Diabetes 2009; 58:1835-43; PMID:19401418; DOI:10.2337/db08-1324.

8. Bertram R, Sherman A, Satin LS. Metabolic and electrical oscillations: partners in controlling pulsatile insulin secretion. Am J Physiol Endocrinol Metab 2007; 293:890-900; PMID:17666486; DOI:10.1152/ajpendo.00359.2007.

9. Bertram R, Sherman A. A calcium-based phantom bursting model for pancreatic islets. Bull Math Biol 2004; 66:1313-44; PMID:15294427; DOI:10.1016/j.bulm.2003.12.005.

10. Magnus G, Keizer J. Minimal model of beta-cell mitochondrial Ca^{2+} handling. Am J Physiol 1997; 273:717-33; PMID:9277370.

11. Magnus G, Keizer J. Model of β-cell mitochondrial calcium handling and electrical activity. I. Cytoplasmic variables. Am J Physiol 1998; 274:1158-73; PMID:9575813.

12. Detimary P, Gilon P, Henquin JC. Interplay between cytoplasmic Ca^{2+} and the ATP/ADP ratio: a feedback control mechanism in mouse pancreatic islets. Biochem J 1998; 333:269-74; PMID:9657965.

13. Civelek VN, Deeney JT, Fusonie GE, Corkey BE, Tornheim K. Oscillations in oxygen consumption by permeabilized clonal pancreatic β-cells (HIT) incubated in an oscillatory glycolyzing muscle extract. Diabetes 1997; 46:51-6; PMID:8971081; DOI:10.2337/diabetes.46.1.51.

14. McCormack JG, Longo E, Corkey B. Glucose-induced activation of pyruate dehydrogenase in isolated rat pancreatic islets. Biochem J 1990; 267:527-30; PMID:2185742.

15. Bertram R, Sherman A. Filtering of calcium transients by the endoplasmic reticulum in pancreatic β-cells. Biophys J 2004; 87:3775-85; PMID:15465863; DOI:10.1529/biophysj.104.050955.

16. Arredouani A, Henquin JC, Gilon P. Contribution of the endoplasmic reticulum to the glucose-induced $[Ca^{2+}]_c$ response in mouse pancreatic islets. Am J Physiol Endocrinol Metab 2002; 282:982-91.

17. Gilon P, Arredouani A, Gailly P, Gromada J, Henquin JC. Uptake and release of Ca^{2+} by the endoplasmic reticulum contribute to the oscillations of the cytosolic Ca^{2+} concentration triggered by Ca^{2+} influx in the electrically excitable pancreatic B-cell. J Biol Chem 1999; 274:20197-205; PMID:10400636; DOI:10.1074/jbc.274.29.20197.

18. Islam MS. Calcium signaling in the islets. In: Islam MS, Ed. The islets of Langerhans. London: Springer 2010; 235-59.

19. Watts M, Tabak J, Zimliki C, Sherman A, Bertram R. Slow variable dominance and phase resetting in phantom bursting. J Theor Biol 2011; 276:218-28; PMID:21315733; DOI:10.1016/j.jtbi.2011.01.042.

20. Diederichs F. Mathematical simulation of membrane processes and metabolic fluxes of the pancreatic β-cell. Bull Math Biol 2006; 68:1779-818; PMID:16832733; DOI:10.1007/s11538-005-9053-9.

21. Fridlyand LE, Tamarina N, Philipson LH. Modeling of Ca^{2+} flux in pancreatic β-cells: role of the plasma membrane and intracellular stores. Am J Physiol Endocrinol Metab 2003; 285:138-54; PMID:12644446.

22. Fridlyand LE, Jacobson DA, Kuznetsov A, Philipson LH. A model of action potentials and fast Ca^{2+} dynamics in pancreatic β-cells. Biophys J 2009; 96:3126-39; PMID:19383458; DOI:10.1016/j.bpj.2009.01.029.

23. Pedersen MG. A biophysical model of electrical activity in human β-cells. Biophys J 2010; 99:3200-7; PMID:21081067; DOI:10.1016/j.bpj.2010.09.004.

24. Keizer J, Smolen P. Bursting electrical activity in pancreatic β cells cause by Ca^{2+} and voltage-inactivated Ca^{2+} channels. Proc Natl Acad Sci USA 1991; 88:3897-901; PMID:1850840; DOI:10.1073/pnas.88.9.3897.

25. Smolen P, Keizer J. Slow voltage inactivation of Ca^{2+} currents and bursting mechanisms for the mouse pancreatic β-cell. J Membr Biol 1992; 127:9-19; PMID:1328645; DOI:10.1007/BF00232754.

26. Smolen P, Terman D, Rinzel J. Properties of a bursting model with two slow inhibitory variables. SIAM J Appl Math 1993; 53:861-92; DOI:10.1137/0153042.

27. Chay TR, Keizer J. Minimal model for membrane oscillations in the pancreatic β-cell. Biophys J 1983; 42:181-90; PMID:6305437; DOI:10.1016/S0006-3495(83)84384-7.

28. Chay TR. Electrical bursting and luminal calcium oscillations in excitable cell models. Biol Cybern 1996; 75:419-31; PMID:8983163; DOI:10.1007/s004220050307.

29. Chay TR. Effects of extracellular clcium on electrical bursting and intracellular and luminal calcium oscillations in insulin secreting pancreatic β-cells. Biophys J 1997; 73:1673-88; PMID:9284334; DOI:10.1016/S0006-3495(97)78199-2.

30. Bertram R, Previte J, Sherman A, Kinard TA, Satin LS. The phantom burster model for pancreatic β-cells. Biophys J 2000; 79:2880-92; PMID:11106596; DOI:10.1016/S0006-3495(00)76525-8.

31. Sherman A, Rinzel J, Keizer J. Emergence of organized bursting in clusters of pancreatic β-cells by channel sharing. Biophys J 1988; 54:411-25; PMID:2850029; DOI:10.1016/S0006-3495(88)82975-8.

32. Sherman A. Contributions of modeling to understanding stimulus-secretion coupling in pancreatic β-cells. Am J Physiol 1996; 271:362-72; PMID:8770032.

33. Tsaneva-Atanasova K, Sherman A. Accounting for near-normal glucose sensitivity in K_{ir} 6.2AAA transgenic mice. Biophys J 2009; 97:2409-18; PMID:19883583; DOI:10.1016/j.bpj.2009.07.060.

34. Bertram R, Satin L, Zhang M, Smolen P, Sherman A. Calcium and glycolysis mediate multiple bursting modes in pancreatic islets. Biophys J 2004; 87:3074-87; PMID:15347584; DOI:10.1529/biophysj.104.049262.

35. Bertram R, Satin LS, Pedersen G, Luciani DS, Sherman A. Interaction of glycolysis and mitochondrial respiration in metabolic oscillations of pancreatic islets. Biophys J 2007; 92:1544-55; PMID:17172305; DOI:10.1529/biophysj.106.097154.

36. Bertram R, Sherman A. Negative calcium feedback: the road from Chay-Keizer. In: Coombes S, Bressloff P, Eds. Bursting: the genesis of rhythm in the nervous system. World Scientific Press 2005; 19-48.

37. Tabak J, Rinzel J, Bertram R. Quantifying the relative contributions of divisive and subtractive feedback to rhythm generation. PLOS Comput Biol 2011; 7:1001124; PMID:21533065; DOI:10.1371/journal.pcbi.1001124.

38. Merrins MJ, Fendler B, Zhang M, Sherman A, Bertram R, Satin L. Metabolic oscillations in pancreatic islets depend on the intracellular calcium level but not calcium oscillations. Biophys J 2010; 99:76-84; PMID:20655835; DOI:10.1016/j.bpj.2010.04.012.

39. Nunemaker CS, Bertram R, Sherman A, Tsaneva-Atanasova K. Glucose modulates calcium oscillations in pancreatic islets via ionic and glycolytic mechanisms. Biophys J 2006; 91:2082-96; PMID:16815907; DOI:10.1529/biophysj.106.087296.

40. Kinard TA, de Vries G, Sherman A, Satin LS. Modulations of the bursting properties of single mouse pancreatic β-cells by artificial conductances. Biophys J 1999; 76:1423-35; PMID:10049324; DOI:10.1016/S0006-3495(99)77303-0.

41. Zhang M, Goforth P, Bertram R, Sherman A, Satin L. The Ca^{2+} dynamics of isolated mouse β-cells and islets: Implications for mathematical models.

42. Ermentrout B. Simulating, analyzing and animating dynamical systems: A guide to XPPAUT for researchers and students. Philadelphia, PA: SIAM 2002.